AD-A131 480 COMPUTATION OF COUNTING DISTRIBUTIONS ARISING FROM A SINGLE-STAGE MULTIPL.. (U) CALIFORNIA UNIV SAN DIEGO LA JOLLA DEPT OF ELECTRICAL ENGINEE.. C W HELSTROM ET AL. 1/1

UNCLASSIFIED 02 MAY 83 AFOSR-TR-83-0677 AFOSR-82-0343 F/G 9/1 NL

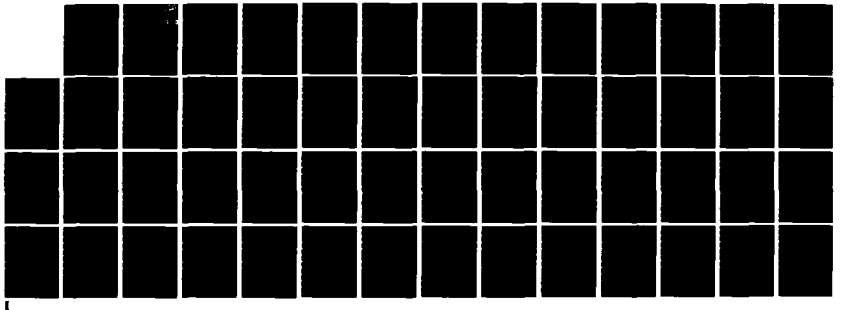

END

FILMED

DTIC

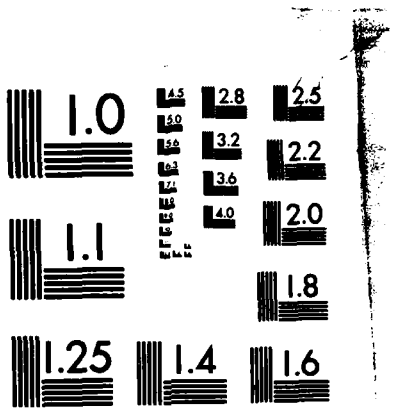

MICROCOPY RESOLUTION TEST CHART
NATIONAL BUREAU OF STANDARDS-1963-A

AFOSR-TR- 83-0677

Computation of Counting Distributions Arising from a Single-Stage Multiplicative Process

Carl W. Helstrom and Stephen O. Rice

Department of Electrical Engineering & Computer Sciences
University of California, San Diego
La Jolla, California, 92093

Abstract

The cumulative distribution of the number of secondary electrons in a single-stage photomultiplier is calculated by numerically integrating the inversion integral for its probability generating function along a suitably chosen contour. A residue series applicable in certain cases is also presented. Saddlepoint approximations to the contour integral are described, which are the more accurate, the greater the numbers of secondaries. Recurrent relations are developed for computing values of the distribution for purposes of comparison. Computation of the Neyman Type-A distribution is treated as a limiting case.

Research sponsored by the Air Force Office of Scientific Research, Air Force Systems Command, USAF under Grant AFOSR-82-0343. The United States Government is authorized to reproduce and distribute reprints for Governmental purposes notwithstanding any copyright notation thereon.

AMS classification 65U05, 60E10

37 MS pages, 7 figs, 7 tables

Unclassified

SECURITY CLASSIFICATION OF THIS PAGE (When Data Entered)

REPORT DOCUMENTATION PAGE		READ INSTRUCTIONS BEFORE COMPLETING FORM
1. REPORT NUMBER **AFOSR-TR- 83-0677**	2. GOVT ACCESSION NO. AD-A131480	3. RECIPIENT'S CATALOG NUMBER
4. TITLE (and Subtitle) COMPUTATION OF COUNTING DISTRIBUTIONS ARISING FROM A SINGLE-STAGE MULTIPLICATIVE PROCESS		5. TYPE OF REPORT & PERIOD COVERED INTERIM
		6. PERFORMING ORG. REPORT NUMBER
7. AUTHOR(s) Carl W. Helstrom and Stephen O. Rice		8. CONTRACT OR GRANT NUMBER(s) AFOSR-82-0343
9. PERFORMING ORGANIZATION NAME AND ADDRESS Department of Elec. Engr. & Comp. Sci. University of California, San Diego La Jolla, CA 92093		10. PROGRAM ELEMENT, PROJECT, TASK AREA & WORK UNIT NUMBERS PE61102F; 2304/A5
11. CONTROLLING OFFICE NAME AND ADDRESS AFOSR/NM Bldg. 410 Bolling AFB DC 20332		12. REPORT DATE May 2, 1983
		13. NUMBER OF PAGES 53
14. MONITORING AGENCY NAME & ADDRESS(if different from Controlling Office)		15. SECURITY CLASS. (of this report) Unclassified
		15a. DECLASSIFICATION/DOWNGRADING SCHEDULE

16. DISTRIBUTION STATEMENT (of this Report)

Approved for public release; distribution unlimited.

17. DISTRIBUTION STATEMENT (of the abstract entered in Block 20, if different from Report)

18. SUPPLEMENTARY NOTES

DTIC COPY INSPECTED 2

Accession For	
NTIS GRA&I	X
DTIC TAB	☐
Unannounced	☐
Justification	
By	
Distribution/	
Availability Codes	
Dist	Avail and/or Special
A	

19. KEY WORDS (Continue on reverse side if necessary and identify by block number)

probability distributions, photomultipliers, particle counting, numerical integration

20. ABSTRACT (Continue on reverse side if necessary and identify by block number)

The cumulative distribution of the number of secondary electrons in a single-stage photomultiplier is calculated by numerically integrating the inversion integral for its probability generating function along a suitably chosen contour. A residue series applicable in certain cases is also presented. Saddlepoint approximations to the contour integral are described, which are the more accurate, the greater the numbers of secondaries. Recurrent relations are developed for computing values of the distribution for purposes of comparison. Computation of the Neyman Type-A distribution is treated as a limiting case.

DD FORM 1 JAN 73 1473 EDITION OF 1 NOV 65 IS OBSOLETE

Unclassified

SECURITY CLASSIFICATION OF THIS PAGE (When Data Entered)

I. Particle Multiplication

(a) Introduction

The particle-counting distributions with whose computation this paper is concerned are exemplified by that of the output of a photomultiplier with a single stage of multiplication. In this device primary photoelectrons, driven out by incident light, are accelerated in an electric field and impinge on a surface from which they eject secondary electrons. Let x_j be the number of secondary electrons ejected by the j-th primary electron. Then if k primary electrons strike the surface during a fixed interval (0, T), the total number of secondary electrons is

$$n = \sum_{j=1}^{k} x_j \tag{1.1}$$

The number k of primary electrons is a random variable with probability generating function (p.g.f.)

$$f(z) = \sum_{k=0}^{\infty} \Pi_k z^k, \tag{1.2}$$

where Π_k is the probability that k primary photoelectrons strike the surface. Let the numbers x_j of secondary electrons be independent and identically distributed random variables with probabilities $\Pr(x_j = m) = p_m^{(s)}$ and p.g.f.

$$g(z) = \sum_{m=0}^{\infty} p_m^{(s)} z^m. \tag{1.3}$$

Then the p.g.f. of the total number n of secondary electrons counted during (0, T) is

$$h(z) = \sum_{n=0}^{\infty} p_n z^n = f(g(z)), \tag{1.4}$$

where p_n is the probability that the total number of secondaries equals n [1].

Although the probability distribution $\{p_n\}$ may be of interest in comparing theory with experiment, the cumulative probabilities

$$Q_n^- = \sum_{m=0}^{n-1} p_m, \qquad n = 1, 2, \ldots$$

$$Q_0^- = 0, \tag{1.5}$$

and their complements

$$Q_n^+ = 1 - Q_n^- = \sum_{m=n}^{\infty} p_m \tag{1.6}$$

are generally more useful because they characterize the performance of devices in which some action is triggered when the number n of particles exceeds a certain bias level. False-alarm and detection probabilities in optical- and particle-detection systems and error probabilities in optical communications are directly related to the cumulative distribution, and it is the computation of this distribution that will be studied here. We call Q_n^- and Q_n^+ the "tail probabilities." Their generating functions are

$$H^-(z) = \sum_{n=0}^{\infty} Q_n^- z^n = \frac{zh(z)}{1-z} \tag{1.7}$$

$$H^+(z) = \sum_{n=0}^{\infty} Q_n^+ z^n = \frac{1-zh(z)}{1-z} \tag{1.8}$$

in terms of the p.g.f. h(z).

Multiplicative processes such as this occur in many other contexts as well. A review has recently been given by Teich [2], who mentions applications to biology, medicine, cosmology, geophysics, and operations research. The probabilities p_n and the tail probabilities Q_n^- and Q_n^+ must usually be determined

by numerical methods, but the conventional ones run into difficulties when the numbers n and their expected value E(n) are large. The number of steps needed to compute p_n generally increases with increasing n, as does the number of terms to be summed in evaluating Q_n^-. Inaccuracy in the individual values of p_n introduces large relative errors into the complementary cumulative probabilities $Q_n^+ = 1 - Q_n^-$ when n much exceeds E(n).

In this paper we shall present methods for computing the tail probabilities that become the more efficient, the greater the numbers n and E(n), and do not require computing the individual probabilities p_n and summing them. The application to the output of a multiplicative process may be regarded as exemplifying methods that are worthy of consideration whenever the p.g.f h(z) of some integer-valued random variable n is known in analytical form and the expected value E(n) and the numbers n for which Q_n^- or Q_n^+ is wanted are large.

The principal method involves suitably deforming the contour of integration in the inversion integrals

$$Q_n^- = \int_{C^-} \frac{z^{-n}h(z)}{1-z} \frac{dz}{2\pi i} \tag{1.9}$$

$$Q_n^+ = \int_{C^+} \frac{z^{-n}h(z)}{z-1} \frac{dz}{2\pi i}, \tag{1.10}$$

where C^- and C^+ initially are closed contours enclosing the origin, but no singularities of the m.g.f. h(z); C^+ encloses the point z = 1, C^- does not; and the contours are traversed counterclockwise. The integration along the deformed contour is evaluated by the trapezoidal rule. The use of numerical contour integration to evaluate cumulative distributions of continuous random variables was treated in [3], and a comment on that paper described its application to cumulative distributions of integer-valued random variables [4].

Besides evaluating the tail probabilities Q_n^- and Q_n^+ by numerical contour integration, we shall show how to approximate them by isolating the contributions to the integrals in (1.9) and (1.10) at the saddlepoints of the integrand. Daniels [5] first demonstrated saddlepoint approximations to probability distributions $\{p_n\}$ of integer-valued random variables. Related to this method is the use of tilted distributions, utilized by Blackwell and Hodges [6], Bahadur and Rao [7], Petrov [8], and Barndorff-Nielsen and Cox [9] to calculate cumulative distributions of sums of independent random variables; see also Van Trees [10]. A different saddle-point approximation, which avoids the use of the error-function integral, was utilized for tail probabilities of integer-valued random variables in [11]. In the present problem the contributions of saddlepoints above and below the real axis in the z-plane must be included in addition to that of the principal one lying on the real axis. We shall evaluate the latter by means of a uniform asymptotic expansion [12]; the contributions of the off-axis saddlepoints are evaluated by the method of [11].

The contour-integral method and its approximations apply whenever the p.g.f. h(z) of the output distribution is known in analytical form, but for the sake of definiteness we shall restrict our discussion to distributions arising when the light ejecting the primary electrons is incoherent light with various simple spectral densities, and the number of secondary electrons ejected by each primary electron is governed by a Poisson distribution. A by-product of our study is an illustration of how the output distribution depends on the product of the bandwidth W of the incident light and the duration T of the counting interval.

We first review methods of computing the probabilities p_n that follow most directly from (1.4) and are useful when the numbers n and E(n) are small, in order to generate accurate values of those probabilities for comparison with the contour-integration and other methods to be presented later.

(b) General Multiplicative Processes

From the p.g.f. h(z) the probabilities p_n can be determined by

$$p_0 = h(0),$$

$$p_n = \frac{1}{n!} \left. \frac{d^n h(z)}{dz^n} \right|_{z=0} = \frac{1}{n!} \left. \frac{d^n}{dz^n} f(g(z)) \right|_{z=0}, \qquad n > 0. \tag{1.11}$$

By means of a formula based on Bell polynomials [10, p.1998], the probability p_n can be written as

$$p_n = \sum_{k=1}^{n} f_k H_{n,k}, \qquad n \geq 1, \tag{1.12}$$

where

$$f_k = \left. \frac{d^k}{dz^k} f(z) \right|_{z=g(0)}, \qquad g(0) = p_0^{(s)}, \tag{1.13}$$

and the $H_{n,k}$ are determined by the recurrent relation

$$H_{n+1,1} = p_{n+1}^{(s)},$$

$$H_{n+1,k+1} = \sum_{m=k}^{n} \left(1 - \frac{m}{n+1}\right) p_{n+1-m}^{(s)} H_{m,k}, \tag{1.14}$$

in terms of the distribution of the number of secondaries per primary photoelectron. In particular

$$H_{n,n} = p_1^{(s)n}/n!. \tag{1.15}$$

(c) Poisson-Distributed Secondaries

When, as we assume henceforth, the distribution of the number of secondaries per primary electron has the Poisson form with mean G, which is called the gain,

$$p_n^{(s)} = G^n e^{-G}/n!, \tag{1.16}$$

the probabilities p_n that the total number of secondaries equals n form what

is called a compound or generalized Poisson distribution [13] and are given by

$$p_n = \sum_{k=0}^{\infty} \Pi_k (kG)^n e^{-kG}/n!. \tag{1.17}$$

The p.g.f. of the output distribution is now

$$h(z) = f(e^{G(z-1)}). \tag{1.18}$$

It follows from Problem 26, p. 47 of Riordan's book [14] that

$$H_{n,k} = G^n \bar{S}(n, k)\, e^{-kG} \tag{1.19}$$

in terms of the modified Stirling numbers of the second kind, $\bar{S}(n, k)$, which obey the recurrent relation

$$\bar{S}(1, 1) = 1, \quad \bar{S}(k, n) = 0, \quad k > n,$$
$$\bar{S}(n+1, k) = [\bar{S}(n, k-1) + k\bar{S}(n, k)]/(n+1). \tag{1.20}$$

In terms of the ordinary Stirling numbers of the second kind these are defined by

$$\bar{S}(n, k) = S(n, k)/n! \tag{1.21}$$

and are introduced in order to avoid overflow in machine computation. Recurrent relations for S(n, k) are given in [14]. In particular

$$\bar{S}(n, 1) = \bar{S}(n, n) = 1/n!. \tag{1.22}$$

As a result the probabilities sought are

$$p_0 = f(e^{-G}),$$

$$p_n = G^n \sum_{k=1}^{n} f_k \bar{S}(n, k)\, e^{-kG}, \quad n > 0, \tag{1.23}$$

in which the derivatives f_k of the p.g.f. $f(z)$ of the primary distribution are evaluated at $z = e^{-G}$. This enables computation of the probabilities p_n by a strictly finite procedure in contrast to the infinite series in (1.17).

When the number n is large, however, the great number of iterated computations required by (1.21-.23) may introduce substantial errors due to rounding off. Greater accuracy can be achieved for large n by utilizing (1.17), replacing n! by Stirling's approximation [15] and writing it as

$$p_n = [2\pi(n+1)]^{-\frac{1}{2}}[B(n+1)]^{-1} \sum_{k=1}^{\infty} \Pi_k \left(\frac{kG}{n+1}\right)^n e^{n+1-kG}, \tag{1.24}$$

where

$$B(z) = \exp\left(\frac{1}{12z} - \frac{1}{360z^3} + O(z^{-5})\right) \tag{1.25}$$

The summation was halted when the terms in (1.24) became insignificant.

II. Primaries Ejected by Incoherent Light

(a) Arbitrary Spectral Density

The incident light is assumed to be quasimonochromatic, linearly polarized, incoherent light with a spectral density $\Phi(\omega)$; the angular frequency ω is measured from the central angular frequency of the light. Because the field of the light is a Gaussian random process, the probability generating function of the distribution of primary photoelectrons is

$$f(z) = \prod_{r=1}^{\infty} [1 - N_p \lambda_r (z-1)]^{-1}, \tag{2.1}$$

where N_p is the mean number of primary electrons [16]. The λ_r are the eigenvalues of the integral equation

$$\lambda \rho(t) = \int_0^T \phi(t-s)\rho(s)\, ds, \tag{2.2}$$

whose kernel

$$\phi(\tau) = \int_{-\infty}^{\infty} \Phi(\omega)\, e^{i\omega\tau}\, d\omega/2\pi \tag{2.3}$$

is the temporal coherence function of the light field and the Fourier transform of the spectral density $\Phi(\omega)$; (0, T) is the interval during which electrons are counted. We assume that the spectral density $\Phi(\omega)$ is normalized so that

$$\sum_{r=1}^{\infty} \lambda_r = 1, \tag{2.4}$$

which requires that

$$T\phi(0) = T \int_0^{\infty} \Phi(\omega)\, d\omega/\pi = 1. \tag{2.5}$$

In terms of the Fredholm determinant

$$D(u) = \prod_{r=1}^{\infty} (1+\lambda_r u) \tag{2.6}$$

associated with the integral equation (2.2), the p.g.f. is

$$f(z) = [D(N_p(1-z))]^{-1} = \prod_{r=1}^{\infty} [1-\lambda_r N_p(z-1)]^{-1} \tag{2.7}$$

By introducing the residue expansion of $[D(u)]^{-1}$ we can write this p.g.f. as

$$f(z) = \sum_{r=1}^{\infty} \frac{\alpha_r}{1-N_p\lambda_r(z-1)} = \sum_{r=1}^{\infty} \alpha_r \left(\frac{1-v_r}{1-v_r z}\right),$$

$$\alpha_r = \frac{\lambda_r}{D'(-1/\lambda_r)} = \prod_{s\neq r} \left(1-\frac{\lambda_s}{\lambda_r}\right)^{-1},$$

$$v_r = \frac{N_p\lambda_r}{1+N_p\lambda_r}, \qquad D'(u) = dD/du. \tag{2.8}$$

Because (1.23) is linear in the derivatives f_k, the probabilities p_n can be considered as a weighted sum of probabilities arising from the individual terms of (2.8),

$$p_n = \sum_{r=1}^{\infty} \alpha_r P_{r,n}, \tag{2.9}$$

with

$$P_{r,n} = P_{r,0} G^n \sum_{k=1}^{n} k!\bar{S}(n,k)\xi_r^k, \qquad n > 0,$$

$$\xi_r = \frac{v_r e^{-G}}{1-v_r e^{-G}}, \qquad P_{r,0} = \frac{1-v_r}{1-v_r e^{-G}} \tag{2.10}$$

Writing

$$P_{r,n} = P_{r,0} \sum_{k=1}^{n} T_{n,k}^{(r)},$$

$$T_{n,k}^{(r)} = G^n k!\, \bar{S}(n, k) \xi_r^{\,k}, \tag{2.11}$$

and using the recurrent relation (1.20) for the modified Stirling numbers, we find a recurrent relation for the terms of (2.11),

$$T_{n+1,k}^{(r)} = \frac{kG}{n+1} (\xi_r T_{n,k-1}^{(r)} + T_{n,k}^{(r)}), \qquad T_{1,1}^{(r)} = G\xi_r. \tag{2.12}$$

The sum in (2.9) is stopped when the terms decrease to the point of insignificance.

(b) Lorentz Spectral Density

For incident light with a Lorentz spectral density, whose normalized form is

$$\Phi(\omega) = \frac{2\mu}{T(\omega^2 + \mu^2)}, \tag{2.13}$$

the p.g.f. f(z) of the primary distribution is given by [17]

$$f(z) = e^m [\cosh w + \tfrac{1}{2}\left(\frac{w}{m} + \frac{m}{w}\right) \sinh w]^{-1},$$

$$w^2 = m^2 + 2N_p m(1 - z), \qquad m = \mu T. \tag{2.14}$$

We denote the square bracket by M(z) and write it in terms of modified spherical Bessel functions $i_n(w)$ obeying the recurrent relation

$$i_{n+1}(w) = i_{n-1}(w) - \frac{2n+1}{w} i_n(w) \tag{2.15}$$

with

$$i_{-1}(w) = \frac{\cosh w}{w}, \qquad i_0(w) = \frac{\sinh w}{w},$$

whereupon

$$M(z) = \frac{m}{2} i_0(w) + w(1 + \frac{1}{2m})\, i_{-1}(w) + \frac{w^2}{2m} i_{-2}(w). \tag{2.16}$$

Then following Bédard [18] we use

$$\frac{d^n}{dz^n} M(z) = \left(-\frac{N_p m}{w}\right)^n \left[\frac{m}{2} i_n(w) + w\left(1 + \frac{1}{2m}\right) i_{n-1}(w) + \frac{w^2}{2m} i_{n-2}(w)\right]$$

$$= (-1)^n M_n(z), \tag{2.17}$$

which defines $M_n(z)$, in Leibnitz's formula

$$\frac{d^n}{dz^n} [f(z)M(z)] = \sum_{r=0}^{n} \binom{n}{r} f_r \frac{d^{n-r}}{dz^{n-r}} M(z) = 0 \tag{2.18}$$

to determine a recurrent relation for the derivatives f_n of $f(z)$,

$$f_n = \sum_{r=0}^{n-1} (-1)^{n-r+1} \binom{n}{r} f_r M_{n-r}(z)/M(z),$$

$$z = e^{-G}, \qquad f_0 = f(z), \qquad w = [m^2 + 2N_p m(1-z)]^{\frac{1}{2}}. \tag{2.19}$$

The probability p_n of counting n secondary electrons during (0, T) when the incident light has a Lorentz spectral density is then calculated by substituting from (2.19) into (1.23). Alternatively, one can calculate the probabilities Π_k in (1.17) and (1.24) by Bédard's method [18], which corresponds to taking $z = 0$ in (2.14-.19).

(c) Negative Binomial Primary Distribution

The primary electron distribution can often be closely approximated by the negative binomial distribution

$$\Pi_k = \frac{(M)_k}{k!} (1-v)^M v^k, \qquad v = \frac{N_p}{N_p + M}, \qquad k = 0, 1, 2, \ldots,$$

$$(M)_k = M(M+1)\ldots(M+k-1) = \frac{\Gamma(M+k)}{\Gamma(M)}, \tag{2.20}$$

in which the number M of degrees of freedom is given by

$$M = T^2|\phi(0)|^2 \Big/ \int_{-T}^{T} (T - |\tau|)|\phi(\tau)|^2 d\tau \tag{2.21}$$

in terms of the temporal coherence function $\phi(\tau)$ of the incident light [16, 19]. For the Lorentz spectral density in (2.13)

$$\phi(\tau) = T^{-1} e^{-\mu|\tau|} \tag{2.22}$$

and

$$M = 2m^2/(2m - 1 + e^{-2m}), \qquad m = \mu T; \tag{2.23}$$

$M \to 1$ as $m \to 0$, $M \to m$ as $m \to \infty$. For $M >> 1$,

$$M \doteq T|\phi(0)|^2 \Big/ \int_{-\infty}^{\infty} |\phi(\tau)|^2 d\tau, \tag{2.24}$$

and M roughly equals the time-bandwidth product WT, where W is the equivalent bandwidth

$$W = \left[\int_{-\infty}^{\infty} \Phi(\omega)\, d\omega/2\pi\right]^2 \Big/ \int_{-\infty}^{\infty} [\Phi(\omega)]^2\, d\omega/2\pi \tag{2.25}$$

of the light. The p.g.f. of this negative binomial distribution is

$$f(z) = \left(\frac{1-v}{1-vz}\right)^M \tag{2.26}$$

and the derivatives of the p.g.f. f(z) in (1.23) are

$$f_k = (M)_k f_0 \left(\frac{v}{1-ve^{-G}}\right)^k, \qquad f_0 = \left(\frac{1-v}{1-ve^{-G}}\right)^M. \tag{2.27}$$

Again using the recurrent relation (1.20) with (1.23) we can write the probability p_n of n secondaries as

$$p_n = p_0 \sum_{k=1}^{n} T_{n,k}, \qquad p_0 = f_0, \tag{2.28}$$

in which the coefficients $T_{n,k}$ obey the recurrent relation

$$T_{n+1,k} = \frac{G}{n+1}\,[(M+k-1)\xi T_{n,k-1} + kT_{n,k}],$$

$$\xi = \frac{ve^{-G}}{1-ve^{-G}}, \qquad T_{1,1} = MG\xi. \tag{2.29}$$

(d) The Neyman Type-A Distribution

When we pass to the limit $M \to \infty$, keeping the mean number N_p of primary electrons fixed, the distribution of primary electrons turns into the Poisson distribution,

$$\Pi_k = N_p{}^k \exp(-N_p)/k!, \tag{2.30}$$

for which the p.g.f. is

$$f(z) = \exp[N_p(z-1)]; \tag{2.31}$$

and the distribution of secondaries becomes by (1.18) the Neyman Type-A distribution [2], whose p.g.f. is

$$h(z) = \exp[N_p(e^{G(z-1)} - 1)] \tag{2.32}$$

and for which the probabilities are most simply computed by Neyman's recurrent relation [20]

$$p_{k+1} = \frac{N_p G e^{-G}}{k+1} \sum_{r=0}^{k} \frac{G^r}{r!}\, p_{k-r}, \tag{2.33}$$

or, for $n \gg 1$, by (1.24-.25) and (2.30).

In order to illustrate the transition to the Neyman Type-A distribution with increasing values of M, we have plotted the probabilities p_n, $n > 0$, in Figs. 1 and 2 for both the negative-binomial primary distribution (solid lines) and the distribution arising from light with a Lorentz spectral density (dashed lines), the equivalent value of m having been determined by solving (2.23).

Where both distributions are not shown, their graphs fell too close to be distinguished. The curves marked '∞' represent the Neyman Type-A distribution. In Fig. 1, $N_p = 2$, $G = 6$; in Fig. 2, $N_p = 6$, $G = 2$. The long tails of the negative-binomial distribution for small values of M carry over to the distribution of the number n of secondary electrons. The negative-binomial distribution is seen, furthermore, to yield a close approximation to the distribution arising from light with a Lorentz spectral density over the entire range $1 \leq M < \infty$, the two coinciding at the extremes $M = 1$ and $M = \infty$, except that the latter drops off to zero slightly less rapidly than the former.

The probabilities p_n having been computed by these methods, the cumulative probability Q_n^- is computed by the summation in (1.5), and its complement Q_n^+ is determined from $1 - Q_n^-$. When the numbers n are large, however, Q_n^- is close to 1, and round-off errors corrupting the probabilities p_n introduce large relative errors into the tail probability Q_n^+. These methods furthermore require storage of more and more numbers and entail more and more additions and multiplications as n and E(n) increase. We therefore turn to methods that enable computation of the tail probabilities Q_n^- and Q_n^+ directly and are the more efficacious, the larger the mean number N_p of primaries and the gain G in the multiplicative process.

III. The Method of Residues

By (1.10), (1.18), and (2.8) the right-hand tail probability Q_n^+ is

$$Q_n^+ = \sum_{r=1}^{\infty} \alpha_r q_{r,n} \tag{3.1}$$

where

$$q_{r,n} = \sum_{m=n}^{\infty} P_{r,m} = \int_{C^+} \frac{z^{-n} h_r(z)}{z-1} \frac{dz}{2\pi i} \tag{3.2}$$

with

$$h_r(z) = (1-v_r)/(1-v_r e^{G(z-1)}), \tag{3.3}$$

the contour C^+ enclosing the origin and the point $z = 1$, but none of the poles of $h_r(z)$, which lie at the points

$$\zeta_k^{(r)} = 1 + G^{-1}(\ln v_r^{-1} + 2k\pi i) \tag{3.4}$$

for all integers k, $-\infty < k < \infty$.

As shown in Appendix A, we can expand the contour C^+ into a rectangle at infinity, provided that we also enclose each pole $\zeta_k^{(r)}$ by a small circle traversed clockwise. The integral around the rectangle vanishes, and we are left with the results of applying the residue theorem to the integrals around each pole, whereupon

$$\begin{aligned} q_{r,n} &= -\sum_{k=-\infty}^{\infty} \operatorname{Res} \frac{z^{-n} h_r(z)}{z-1}\Bigg|_{z=\zeta_k^{(r)}} \\ &= G^{-1}(1-v_r) \sum_{k=-\infty}^{\infty} \frac{\zeta_k^{(r)-n}}{\zeta_k^{(r)} - 1} \\ &= G^{-1}(1-v_r)\left[\frac{\zeta_0^{(r)-n}}{\zeta_0^{(r)}-1} + 2\,\mathrm{Re}\sum_{k=1}^{\infty} \frac{\zeta_k^{(r)-n}}{\zeta_k^{(r)}-1}\right]. \end{aligned} \tag{3.5}$$

It is furthermore shown in Appendix A that the error R_K incurred by stopping the summation in (3.5) at $k = K$ is bounded by

$$|R_K| \leq \pi^{-1}(1 - v_r)\gamma_n \left[\frac{G}{\pi(2K+1)}\right]^n, \tag{3.6}$$

$$\gamma_n = \pi^{\frac{1}{2}}\Gamma\left(\frac{n-1}{2}\right)/\Gamma(n/2). \tag{3.7}$$

The factors γ_n remain bounded and are of order $n^{-\frac{1}{2}}$ for $n \gg 1$. When n is large, only a few terms contribute significantly to the sum in (3.5), and convergence is rapid.

For the Lorentz spectral density in (2.13), to which we have applied this method, the eigenvalues λ_r are given by

$$\lambda_r = \frac{2m}{c_r^2 + m^2}, \qquad m = \mu T, \tag{3.8}$$

where the c_r are the solutions of the transcendental equation

$$\cot c_r = (c_r^2 - m^2)/2mc_r, \qquad r = 1, 2, \ldots,$$

which can also be written

$$\begin{aligned} c_r \tan (c_r/2) &= m, \qquad r \text{ odd} \\ c_r \cot (c_r/2) &= -m, \qquad r \text{ even} \end{aligned} \tag{3.9}$$

The quantity c_r lies between $(r-1)\pi$ and $r\pi$, and with $c_r = (r-1)\pi + \varepsilon_r$, we find for $r \gg m/\pi$,

$$\varepsilon_r \cong 2m/r\pi. \tag{3.10}$$

The coefficients α_r in (2.8), (2.9), and (3.1) are given by [21]

$$\alpha_r = m^{-1} e^m \sin c_r \left(\frac{(-1)^{r-1}}{\sin c_r} + c_r^{-1}\right)^{-1},$$

which after some algebra can be reduced to

$$\alpha_r = (-1)^{r-1} e^m \lambda_r (2 - m\lambda_r)/(1 + \lambda_r). \tag{3.11}$$

For large values of r, by (3.11) and (3.8)

$$|\alpha_r| \cong 4me^m/r^2\pi^2, \tag{3.12}$$

which decreases in proportion to r^{-2} as $r \to \infty$. This rapid decrease does not set in, however, until r exceeds m/π. When $m \gg 1$, the coefficients α_r for $r < m/\pi$ are large in absolute value; they always alternate in sign. When the number n is of the order of E(n) or larger, the convergence of (3.1) is accelerated by the rapid decrease of the terms $\zeta_k^{(r)-n}$ in (3.5) with increasing r, but for $n \ll E(n)$ many terms of the series must be taken when $m \gg 1$. Because the terms of (3.1) are of decreasing magnitude and alternate in sign, the error is bounded by the last term included in the sum.

In Table I we compare the results of using (3.1) and (3.5) with those obtained by summing the probabilities calculated by (1.23) with (2.19) in double precision. The column headed "last increment" lists the last term added into the sum in (3.1). We took $m = 4.4365821$, corresponding to $M = 5$ in (2.23), and forty terms of (3.1) were summed. For these we found

$$Q_0^+ = \sum_{r=1}^{40} \alpha_r = 1.046101$$

instead of 1. It is seen that the error incurred by the residue series decreases with increasing n, and the faster, the smaller the gain G.

When the p.g.f. f(z) of the primary electrons can be approximated as in (2.26) for integral values of M, the p.g.f.

$$h(z) = \left(\frac{1-v}{1-ve^{G(z-1)}}\right)^M \tag{3.13}$$

possesses a vertical row of poles of order M at the points

$$\zeta_k = 1 + G^{-1}(\ln v^{-1} + 2k\pi i), \qquad -\infty < k < \infty. \tag{3.14}$$

Expanding the contour of integration across this row of poles and applying the residue theorem as before yields for the complementary cumulative probability

$$Q_n^+ = \frac{-1}{(M-1)!} \sum_{k=-\infty}^{\infty} \frac{d^{M-1}}{dz^{M-1}} \left[(z-\zeta_k)^M \frac{z^{-n} h(z)}{z-1} \right] \Bigg|_{z=\zeta_k} \tag{3.15}$$

It is shown in Appendix B that this can be written as

$$Q_n^+ = \frac{(1-v)^M}{G} \sum_{k=-\infty}^{\infty} \frac{\zeta_k^{-n}}{\zeta_k - 1} \sum_{j=0}^{M-1} \sigma_j^{(M)} G^{-j} E_{kj} \tag{3.16}$$

with

$$E_{kj} = (\zeta_k - 1)^{-j} \sum_{s=0}^{j} \frac{(n)_s}{s!} (1 - \zeta_k^{-1})^s, \tag{3.17}$$

$$(n)_s = n(n+1)\ldots(n+s-1), \tag{3.18}$$

and the coefficients $\sigma_j^{(M)}$ are tabulated in Table II. The manner of calculating these coefficients is given in Appendix B. Again the symmetry of the poles about the real axis permits carrying the summation from k = 0 to ∞ and replacing the terms with k > 0 by twice their real parts.

Table III compares the results of this residue series with the exact probabilities for M = 5 and the same parameters as in Table I. The column labeled 'Num' lists the maximum value of k in eq. (3.16), in which the summation was stopped when the ratio of the absolute value of the last term to that of the sum fell below 10^{-6}. This is of the order of magnitude of the discrepancy between the exact values, computed by (2.28 - .29), and those computed by (3.16). As is to be expected from (3.6), the number of terms to be summed decreases with increasing n. The column of Table III headed "Single term" lists the contribution of the pole ζ_0 on the real axis alone: for n greater than E(n) it is seen to provide an accurate approximation to the right-hand tail probability Q_n^+.

IV. Numerical Contour Integration

The method of residues in Sec. III cannot be applied to the Neyman Type-A distribution, whose p.g.f. has no poles, nor to the distribution of secondaries arising from primaries with a negative-binomial distribution for a nonintegral value of M, for which the singularities are branch points. For light with a spectral density such as the Lorentz in (2.13), furthermore, (3.1) requires a great many terms when WT >> 1 and n << E(n) in order to determine $Q_n^- = 1 - Q_n^+$ with usefully high relative accuracy. We therefore resort to computing the tail probabilities Q_n^- and Q_n^+ by evaluating the contour integrals in (1.9) and (1.10) numerically.

For the sake of efficiency one would like to integrate along that contour C on which the magnitude of the integrand decreases as rapidly as possible from its maximum value, which occurs for z real and positive. Such a path is known as the path of steepest descent [22]. With the integrand written in the form

$$\exp[\Psi(z)] = \pm z^{-n} h(z)/(z-1), \tag{4.1}$$

the imaginary part $\mathrm{Im}\Psi(z)$ of the "phase" $\Psi(z)$ is constant along this path. The path of steepest descent furthermore passes through the saddlepoints of the integrand, which are the points at which

$$\frac{d\Psi}{dz} = \frac{d}{dz} \ln h(z) - \frac{n}{z} - \frac{1}{z-1} = 0. \tag{4.2}$$

If one plots the magnitude of the integrand $\exp[\Psi(x)]$ for values of $z = x$ on the positive real axis, one finds that it is a convex function with one minimum at a point x_0^- in $0 < x < 1$ and another at a point x_0^+ in $1 < x < \gamma_0$, where γ_0 is the leftmost singularity of h(z) on the real axis. These points $z = x_0^\pm$ are roots of (4.2) and the principal saddlepoints of the integrand. When the contour of integration passes vertically through $z = x_0^-$ or $z = x_0^+$, the magnitude of the integrand, maximum at the saddlepoint, decreases most rapidly on

either side.

Figure 3 exhibits typical paths of steepest descent for (1.9) and (1.10) when these are used to calculate the Neyman Type-A distribution, whose p.g.f. h(z) is given in (2.32). They are drawn for $N_p = G = 10$. Only the curves in the upper half-plane are illustrated; the portions in the lower half-plane are their mirror images. The left-hand set of curves refers to Q_n^- for n = 75, the right-hand set to Q_n^+ for n = 150. Small circles indicate the saddlepoints. The paths of steepest descent go off to infinity along asymptotes at values of y = Im z equal to odd multiples of π/G.

Utilizing the path of steepest descent would require computing a number of saddlepoints z_0 by solving (4.2) and then tracing the branch of the path of steepest descent passing through each, a cumbersome procedure. We therefore instead chose as our contour of integration a vertical straight line passing through the saddlepoint x_0^- for Q_n^- and through x_0^+ for Q_n^+. This line passes close to the saddlepoints of the integrand lying above and below the real axis. (The advantages of integrating along a path passing through or near a string of saddlepoints were pointed out by Lugannani and Rice [23].)

The saddlepoints x_0^- and x_0^+ on the real axis can most expeditiously be found by solving (4.2) by Newton's method, starting with an initial trial value just to the left of z = 1 for x_0^- and just to the right of z = 1 for x_0^+; at each stage one replaces the trial value x_0' by

$$x_0' + x_0' - \Psi'(x_0')/\Psi''(x_0'), \tag{4.3}$$

with Ψ' the first, Ψ'' the second derivative of the phase $\Psi(x)$; see (4.1). Along a vertical contour through x_0^- or x_0^+ the magnitude of the integrand in (1.9) or (1.10) decreases most rapidly. For $n < E(n)$ it is most expeditious to evaluate Q_n^- in (1.9) by deforming the contour into a straight line through the left-hand

saddlepoint x_0^- ; for $n > E(n)$ one evaluates Q_n^+ by (1.10) and deforms the contour into a straight line through the right-hand saddlepoint x_0^+.

For reasons discussed in [24] the trapezoidal rule is recommended for infinite integrals of analytic functions. For $z = x_0 + iy$ in the neighborhood of the saddlepoint $x_0 = x_0'$ or x_0'' the integrand has approximately a Gaussian dependence on y with a width of the order of $[\Psi''(x_0)]^{-\frac{1}{2}}$. Using the trapezoidal rule in the form

$$Q_n^{\pm} = (\Delta/\pi)\left\{\tfrac{1}{2}\exp\Psi(x_0) + \mathrm{Re}\sum_{k=1}\exp[\Psi(x_0 + ik\Delta)]\right\}, \tag{4.4}$$

it is convenient initially to take the step-size Δ as $[\Psi''(x_0)]^{-\frac{1}{2}}$ and to repeat the integration with values of Δ successively halved until the value of the integral ceases changing significantly [3, 24].

After the initial descent, the integrand in (1.9) and (1.10) may oscillate. The magnitude of these oscillations is measured by $\exp[\mathrm{Re}\Psi(z)]$, and the integration should continue until this magnitude is sufficiently small. The truncation error $\mathcal{E}$ incurred by halting the integration at a particular value y_0 of y is bounded by

$$\mathcal{E} = \left|\int_{y_0}^{\infty}\exp\Psi(x_0 + iy)\,dy/\pi\right| \le \pi^{-1}\max_y|h(x_0+iy)|\int_{y_0}^{\infty}\frac{r^{-n}}{|z-1|}\,dy$$

$$\le \pi^{-1}\max_y|h(x_0+iy)|\int_{y_0}^{\infty}(x_0^2+y^2)^{-n/2}\,dy/y$$

$$= \pi^{-1}\max_y|h(x_0+iy)|\int_{r_0}^{\infty}\frac{r^{-(n-1)}}{r^2-x_0^2}\,dr$$

$$\le \pi^{-1}\,r_0^{-(n-2)}y_0^{-2}\max_y|h(x_0+iy)|/(n-2), \tag{4.5}$$

where $r_0 = (x_0^2 + y_0^2)^{\frac{1}{2}}$.

For the Neyman Type-A distribution,

$$\max_y |h(x_0 + iy)| = \exp [N_p(e^{G(x_0-1)} - 1)]$$

and for that arising from a negative-binomial primary distribution, by (2.26) and (1.18),

$$\max_y |h(x_0 + iy)| = (1-v)^M [1 - v \exp G(x_0 - 1)]^{-M}.$$

The final bracket is positive because the saddlepoint x_0 lies to the left of the leftmost pole of $h(z)$ as given by (3.14) with $k = 0$.

Tables IV and V show results of our computation of the Neyman Type-A distribution and of that arising from a negative-binomial primary distribution with $M = 5$. The summations were halted when the ratio of the bound on the truncation error, as given by (4.5), to the computed probability fell below 10^{-7}. The column headed "Exact" was computed by summing probabilities p_n calculated in double precision from (1.17) with (2.30) and (2.20) respectively, and because of round-off error in our computer, which even in double precision carries only about sixteen decimal digits, the numerical integrations had to be carried out in double precision as well. The numerical contour integration in these examples yielded the tail probabilities to six significant figures with fewer than two hundred steps.

In Figs. 4 and 5 we exhibit the cumulative distribution for the parameters used in Tables IV and V: $N_p = 5$, $G = 20$ and $N_p = 20$, $G = 5$, respectively, and for $M = 1$, 3, 5, 10, and ∞, the mean $N_pG = 100$ remaining fixed. The figures illustrate the manner in which the Neyman Type-A distribution ($M = \infty$) is approached with increasing M. Figs. 6 and 7 exhibit the same cumulative distributions, but for $N_p = 18$, $G = 72$ and $N_p = 72$, $G = 18$, respectively, the mean $N_pG = 1296$

remaining fixed. Comparison with Figs. 4 and 5 shows the approach of the Neyman Type-A distribution to normality as the mean $N_p G$ increases, as predicted by Teich [2]. The distributions arising from the negative-binomial primary distribution manifest no such progression toward normality.

The small circles in Figs. 4 to 7 mark the values of the cumulative distribution of secondary electrons arising from incident light with a Lorentz spectral density; these were computed by the residue series in Sec. III. For a few sets of values the numerical integration method of this section was also carried out, and results agreed. The tails of this distribution do not drop off to zero so rapidly as for the approximating distribution calculated from the negative-binomial primary distribution with the same number M of degrees of freedom, as specified by (2.23). The latter corresponds to a spectral density that cuts off sharply at a frequency deviation of the order of $W = M/T$ from the central frequency of the light; the Lorentz spectrum, on the other hand, has very long tails. Because very large frequency deviations are much more prevalent in the latter, there are more opportunities for large count deviations to be accumulated, and numbers n much larger or much smaller than the mean E(n) are therefore more probable than with primaries having a negative-binomial distribution.

V. Saddlepoint Approximations

The principal contributions to the integrals in (1.9) and (1.10), after the contours have been deformed into the paths of steepest descent as discussed in Sec. IV, come from the neighborhood of each saddlepoint z_k; these saddlepoints are the roots of (4.2). The integrals can then be approximated by

$$Q_n^{\pm} \cong Q_n^{\pm(0)} + 2\ \mathrm{Re} \sum_{k=1}^{\infty} [2\pi\Psi''(z_k)]^{-\frac{1}{2}} \exp[\Psi(z_k)](1+C_k), \tag{5.1}$$

where $Q_n^{\pm(0)}$ represents the contribution of the branch of the path of steepest descent passing through a saddlepoint on the real axis; z_1, z_2, ..., are saddlepoints lying above the real axis, and C_k is a complex correction term given by

$$C_k = \frac{1}{8}(\kappa_4 - \frac{5}{3}\kappa_3^2),$$

$$\kappa_m = \Psi^{(m)}(z_k)/[\Psi^{(2)}(z_k)]^{m/2},\ \Psi^{(m)}(z) = d^m\Psi(z)/dz^m, \tag{5.2}$$

In (5.1) we must take $\mathrm{Re}\,[\Psi''(z_k)]^{\frac{1}{2}} > 0$. Since the contributions of the complex saddlepoints are usually much smaller than $Q_n^{\pm(0)}$, it is often unnecessary to include the correction C_k. Occasionally, however, C_k may have a strong influence if the principal term that $(1+C_k)$ multiplies has a phase close to $\pm\pi/2$, so that without the factor $(1+C_k)$ its real part would be small. The saddlepoints z_k must be determined with high precision.

One method of approximating the on-axis term $Q_n^{\pm(0)}$ is to use the counterpart of (5.1-.2) [9],

$$Q_n^{\pm(0)} \cong [2\pi\Psi^{(2)}(x_0)]^{-\frac{1}{2}} \exp\Psi(x_0)$$
$$\times\left\{1 + \frac{1}{8}\left[\frac{\Psi^{(4)}(x_0)}{[\Psi^{(2)}(x_0)]^2} - \frac{5}{3}\frac{[\Psi^{(3)}(x_0)]^2}{[\Psi^{(2)}(x_0)]^3}\right]\right\} \tag{5.3}$$

with $x_0 = x_0^-$ for $Q_n^{-(0)}$ and $x_0 = x_0^+$ for $Q_n^{+(0)}$, where x_0^- and x_0^+ are the

real-axis saddlepoints defined in Sec. IV. This approximation is the more accurate, the farther the value of n lies from the mean E(n) of the distribution.

For n near E(n) greater accuracy is achieved by utilizing the first two terms of a uniform asymptotic expansion [12, 25]. It is based on the modified phase

$$\tilde{\Psi}(z) = \ln h(z) - n \ln z,$$

of which a saddlepoint $\tilde{x}_0$ is the root of

$$\tilde{\Psi}'(z) = \frac{h'(z)}{h(z)} - \frac{n}{z} = 0. \tag{5.4}$$

This saddlepoint $z = \tilde{x}_0$ can also be quickly computed by Newton's method. There is a single such saddlepoint on the real axis, $0 < \tilde{x}_0 < \gamma_0$, where γ_0 is the leftmost singularity of h(z) on the real axis. At the point $x = \tilde{x}_0$, $\tilde{\Psi}(x)$ is minimum.

The contour of integration is displaced from the path of steepest descent of the entire integrand so that it coincides with that of the function $\exp \tilde{\Psi}(z)$, which lies nearby. Then the first two terms of the uniform asymptotic expansion [25] approximate the tail probabilities as

$$\left.\begin{array}{ll} n > E(n): & Q_n^{+(0)} \\ n < E(n): & Q_n^{-(0)} \end{array}\right\} \cong \operatorname{erfc}\,[-2\tilde{\Psi}(\tilde{x}_0)]^{\frac{1}{2}}$$

$$+ \{|\tilde{x}_0 - 1|^{-1}[2\pi\tilde{\Psi}''(\tilde{x}_0)]^{-\frac{1}{2}} - \tfrac{1}{2}[-\pi\tilde{\Psi}(\tilde{x}_0)]^{-\frac{1}{2}}\} \exp\,[\tilde{\Psi}(\tilde{x}_0)], \tag{5.5}$$

in which primes indicate differentiation and

$$\operatorname{erfc} u = (2\pi)^{-\frac{1}{2}} \int_x^\infty \exp\,(-t^2/2)\, dt$$

is the error-function integral. Corrections of higher order are listed in [25]. For $n = E(n) = N_p G$, $x_0 = 1$ and this approximation breaks down, but by Eq. (17) of [25] we can write for $n = E(n) = \bar{n}$

$$Q_n^{+(0)} \cong \frac{1}{2} - \frac{1}{6}[2\pi\Psi''(1)]^{-\frac{1}{2}}\Psi'''(1)/\Psi''(1); \tag{5.6}$$

further terms are to be found in [25]. Thus for the Neyman Type-A distribution

$$Q_n^{+(0)} \cong \frac{1}{2} - \frac{1}{6}[2\pi\bar{n}(G+1)]^{-\frac{1}{2}}\left(\frac{G^2-2}{G+1}\right) \tag{5.7}$$

and for the distribution of secondaries generated by primaries with a negative-binomial distribution

$$Q_n^{+(0)} \cong \frac{1}{2} - \frac{1}{6}\left\{2\pi\bar{n}[G(1+\nu)+1]\right\}^{-\frac{1}{2}}\left[\frac{G^2(1+3\nu+2\nu^2)-2}{G(1+\nu)+1}\right],$$

$$\nu = N_p/M. \tag{5.8}$$

In Tables VI and VII we compare the results of the saddlepoint approximation with the exact values of the cumulative distribution; Table VI refers to the Neyman Type-A distribution, Table VII to that arising from the negative-binomial primary distribution. The column marked "UAE" was computed from (5.5) or -- for $n = N_p G$ -- from (5.6). The "off-axis contribution" is the summation in (5.1) over the four nearest complex saddlepoints z_1, z_2, z_3, and z_4, including the correction C_k, which amounted to a few percent. This contribution is the larger, the smaller n; for $n > E(n)$ it is hardly significant. The smaller the gain G, the farther the complex saddlepoints lie from the real axis, and the less they contribute to the total probability Q_n^- or Q_n^+. The column labeled "crude SP" lists the value of $Q_n^{\pm(0)}$ computed from (5.3), omitting the factor in brackets. This is the most simply calculated of approximations to these probabilities and is often adequate when n lies far in the tails of the distribution $N_p \gg 1$, $G \gg 1$. It can be useful, for instance, in initial search for the level n yielding a particular value of Q_n^- or Q_n^+, as in setting a bias level to attain a pre-assigned false-alarm probability, or "size", in a hypothesis test.

Conclusion

Three methods have been presented for calculating the cumulative distribution Q_n^- and the complementary distribution Q_n^+ of the number n of secondaries in a particle-multiplication process. They are appropriate when the number n and its mean value $E(n) = N_p G$ are so large that the recurrent computations of Sec. I are infeasible. When the probability generating function h(z) has poles whose locations and residues can be determined, the residue series of Sec. III is the most efficient for $n \gtrsim E(n)$. For $n < E(n)$ in these cases, and in general when a residue expansion cannot be applied -- as for the negative-binomial primary distribution with M nonintegral, and for the Neyman Type-A distribution -- the numerical integration method of Sec. IV can be made as accurate as desired by using sufficiently small steps. If approximations suffice, the saddlepoint methods of Sec. V can be utilized, but one must in general include the contributions of saddlepoints above and below the real axis in addition to that of the principal saddlepoint on the real axis.

Acknowledgment

We wish to thank Mr. James Ritcey for programming the computations leading to the curves in Figs. 1 and 2 for the Lorentz spectral density.

Appendix A. Convergence of Residue Series

We expand the contour C_+ in (3.2) into a rectangle with vertical sides at $x = \pm\infty$ and with horizontal sides along the lines $z = x \pm iy_K$, where

$$y_K = 2\pi(K+\tfrac{1}{2})/G, \qquad -\infty < x < \infty. \tag{A.1}$$

In the course of its expansion the contour crosses the line of poles at $\zeta_k^{(r)}$, $-K \le k \le K$, and leaves behind it a little circle surrounding each pole.

The vertical sides of the rectangle contribute zero to the integral around it because of the factor z^{-n} in the integrand. The contributions from the little circles are evaluated by the residue theorem as in Sec. 3, and we obtain for (3.2)

$$q_{r,n} = q_{r,n}^{(K)} + R_K \tag{A.2}$$

with

$$q_{r,n}^{(K)} = \frac{1-v_r}{G} \sum_{k=-K}^{K} \frac{\zeta_k^{(r)-n}}{\zeta_k^{(r)} - 1}, \tag{A.3}$$

$$R_K = I_+ + I_-, \tag{A.4}$$

where

$$I_+ = \int_{\infty+iy_K}^{-\infty+iy_K} \frac{z^{-n}\, h_r(z)}{z-1} \frac{dz}{2\pi i}, \tag{A.5}$$

$$I_- = \int_{-\infty-iy_K}^{\infty-iy_K} \frac{z^{-n}\, h_r(z)}{z-1} \frac{dz}{2\pi i} = I_+^*. \tag{A.6}$$

We want to bound the remainder term R_K.

Along the upper side of the rectangle, $z = x + iy_K$, $-\infty < x < \infty$,

$$e^{G(z-1)} = \exp[G(x-1) + 2\pi(K+\tfrac{1}{2})i] = -e^{G(x-1)},$$

and

$$h_r(z) = \frac{1-v_r}{1+v_r e^{G(x-1)}} \le 1-v_r. \tag{A.7}$$

Hence

$$|I_+| = \left| \int_{-\infty}^{\infty} \frac{h_r(x+iy_K)dx}{2\pi(x-1+iy_K)(x+iy_K)^n} \right|$$

$$\le \frac{(1-v_r)}{2\pi} \int_{-\infty}^{\infty} \frac{dx}{|x-1+iy_K|(x^2+y_K^2)^{n/2}} \tag{A.8}$$

and since

$$|x-1+iy_K|^{-1} \le y_K^{-1},$$

we find

$$|I_+| \le \frac{1-v_r}{2\pi y_K} \int_{-\infty}^{\infty} (x^2+y_K^2)^{-n/2}\, dx$$

$$= \frac{1-v_r}{2\pi} y_K^{-n} \int_{-\pi/2}^{\pi/2} \cos^{n-2}\theta\, d\theta$$

$$= \frac{1-v_r}{2\pi} \gamma_n y_K^{-n} \tag{A.9}$$

with γ_n given by (3.7). Thus the remainder term is bounded by

$$|R_K| = |2\,\mathrm{Re}\, I_+| \le 2|I_+|$$

$$\le \pi^{-1}(1-v_r)\gamma_n\left(\frac{G}{\pi(2K+1)}\right)^n. \tag{A.10}$$

The same bound applies to the error incurred by cutting off the summation in (3.16) at $k = -K$ and $k = K$, with $(1-v_r)$ replaced by $(1-v)^M$, as can easily be shown by replacing $h_r(z)$ in (A.7) with $h(z)$ in (3.13).

In this way we show that the partial sums in (A.3) converge to the probabilities $q_{r,n}$ defined in (3.2) and summed in (3.1). The convergence of the

series in (3.1) follows from Abel's criterion [26]. The series

$$Q_0^+ = \sum_{r=1}^{\infty} \alpha_r \tag{A.11}$$

converges to 1 by virtue of (2.8) with $z = 1$; $f(1) = 1$ by (2.7). We need only to show that for r sufficiently large, the $q_{r,n}$ form a monotonely decreasing sequence in r for fixed n. Now by (2.20), (2.26), and (1.17) with $v = v_r$, $M = 1$, the quantities $P_{r,m}$ defined by (2.8) and (2.9) are

$$P_{r,m} = (1 - v_r) \sum_{k=1}^{\infty} v_r^{\,k} (kG)^m e^{-kG}/m! \tag{A.12}$$

The eigenvalues λ_r of (2.2) and hence the v_r defined in (2.8) are arranged in descending order, and $v_r \to 0$ as $r \to \infty$. For some integer r_0, $v_r < \frac{1}{2}$ for all $r > r_0$, whereupon

$$(1 - v_r)v_r^{\,k} > (1 - v_{r+1})v_{r+1}^{\,k}, \qquad r > r_0, \ \forall k \geq 1,$$

and the probabilities $(1 - v_r)v_r^{\,k}$ in (A.12) form a monotonely decreasing sequence. The probabilities $P_{r,m}$, therefore, form such a sequence, and so do the probabilities

$$q_{r,n} = \sum_{k=m}^{\infty} P_{r,m}$$

Since the series in (A.11) converges, and for $r > r_0$ the $q_{r,n}$ form a monotonely decreasing sequence, the series in (3.1) converges by Abel's criterion.

Appendix B. Residue Expansion

Dropping the subscript k, we write the terms in (3.15), with (3.13), as

$$\text{Res} = \frac{-1}{(M-1)!}\ \frac{d^{M-1}}{dz^{M-1}}\left[\frac{(1-v)^M(z-\zeta)^M z^{-n}}{\left(1-e^{G(z-\zeta)}\right)^M(z-1)}\right]\Bigg|_{z=\zeta}$$

$$= -\frac{(1-v)^M}{(M-1)!}\ \frac{d^{M-1}}{dz^{M-1}}\left[F(z)\ G(z)\right]\Bigg|_{z=\zeta} \tag{B.1}$$

with

$$F(z) = \left[\frac{z-\zeta}{1-e^{G(z-\zeta)}}\right]^M, \quad G(z) = \frac{z^{-M}}{z-1} \tag{B.2}$$

so that

$$\text{Res} = -\frac{(1-v)^M}{(M-1)!}\sum_{r=0}^{M-1}\binom{M-1}{r}\frac{d^{M-1-r}}{dz^{M-1-r}}F(z)\ \frac{d^r}{dz^r}G(z)\Bigg|_{z=\zeta}$$

$$= -(1-v)^M\sum_{r=0}^{M-1}\Phi_{M-1-r}\Gamma_r \tag{B.3}$$

with

$$\Phi_r = \frac{1}{r!}\ \frac{d^r}{dz^r}F(z)\Bigg|_{z=\zeta} \tag{B.4}$$

$$\Gamma_r = \frac{1}{r!}\ \frac{d^r}{dz^r}G(z)\Bigg|_{z=\zeta} \tag{B.5}$$

Starting with Φ_r, we put into F(z) in (B.2)

$$G(z-\zeta) = y,$$

so that

$$\Phi_r = \frac{(-1)^M G^{r-M}}{r!}\ \frac{d^r}{dy^r}\left[\left(\frac{e^y-1}{y}\right)^{-M}\right]\Bigg|_{y=0} \tag{B.6}$$

Now we apply the method of Bell polynomials as in (1.11) - (1.15), except that here

$$f(z) = z^{-M}, \qquad g(z) = \frac{e^z - 1}{z} \tag{B.7}$$

The k-th derivative of f(z) is

$$f_k = (-1)^k (M)_k \, z^{-(M+k)},$$

$$(M)_k = M(M+1)\ldots(M+k-1),$$

$$z = g(0) = 1, \tag{B.8}$$

and as in (1.12),

$$\Phi_r = (-1)^M G^{r-M} \sum_{k=1}^{r} f_k H_{r,k} \tag{B.9}$$

with the $H_{r,k}$ obeying the recurrent relation [12]

$$H_{r+1,k+1} = \frac{1}{r+1} \sum_{m=k}^{r} \frac{g_{r+1-m}}{(r-m)!} H_{m,k},$$

$$H_{r,1} = \frac{g_r}{r!}, \qquad H_{r,r} = g_1{}^r/r! \tag{B.10}$$

in which

$$g_k = \frac{d^k}{dz^k} g(z)\bigg|_{z=0} = \frac{1}{k+1} \tag{B.11}$$

Thus we obtain

$$\Phi_r = (-1)^M G^{r-M} \sum_{k=1}^{r} (-1)^k (M)_k H_{r,k} \tag{B.12}$$

in which the $H_{r,k}$ are given by the recurrent relation

$$H_{r+1,k+1} = \frac{1}{r+1} \sum_{m=k}^{r} \frac{H_{m,k}}{(r-m)!\,(r+2-m)}$$

$$= \frac{1}{r+1} \sum_{j=0}^{r-k} \frac{H_{r-j,k}}{j!\,(j+2)} \tag{B.13}$$

with special values

$$H_{1,1} = \frac{1}{2}, \quad H_{r,1} = \frac{1}{(r+1)!}, \quad H_{r,r} = \frac{1}{2^r r!} \tag{B.14}$$

For Γ_r in (B.5) we obtain

$$\Gamma_r = \frac{1}{r!} \left. \frac{d^r}{dz^r} z^{-n}(z-1)^{-1} \right|_{z=\zeta}$$

$$= \frac{1}{r!} \sum_{s=0}^{r} \binom{r}{s} \frac{d^s}{dz^s} (z^{-n}) \frac{d^{r-s}}{dz^{r-s}} (z-1)^{-1} \Bigg|_{z=\zeta}$$

$$= (-1)^r \sum_{s=0}^{r} \binom{n+s-1}{s} \frac{\zeta^{-(n+s)}}{(\zeta-1)^{r-s+1}}$$

$$= (-1)^r \frac{\zeta^{-n}}{(\zeta-1)^{r+1}} \sum_{s=0}^{r} \binom{n+s-1}{s} \left(\frac{\zeta-1}{\zeta}\right)^s \tag{B.15}$$

It is convenient to write

$$-\Phi_r = (-1)^{M-1-r} G^{-1} G^{-(M-r-1)} T_r^{(M)}, \tag{B.16}$$

with

$$T_r^{(M)} = (-1)^r \sum_{k=1}^{r} (-1)^k (M)_k H_{r,k},$$

$$T_0^{(M)} = 1, \qquad 0 \le r \le M-1, \tag{B.17}$$

whereupon, with

$$\Gamma_r = (-1)^r \frac{\zeta^{-n}}{\zeta - 1} (\zeta - 1)^{-r} \sum_{s=0}^{r} \binom{n+s-1}{s} \left(\frac{\zeta - 1}{\zeta}\right)^s \tag{B.18}$$

we find from (B.3)

$$\text{Res} = \frac{(1-v)^M}{G} \sum_{r=0}^{M-1} (-1)^r G^{-r} T_{M-1-r}^{(M)} \Gamma_r$$

$$= \frac{(1-v)^M}{G} \sum_{j=0}^{M-1} \sigma_j^{(M)} G^{-j} E_j \frac{\zeta^{-n}}{\zeta - 1} \tag{B.19}$$

$$E_j = (\zeta - 1)^{-j} \sum_{s=0}^{j} \frac{(n)_s}{s!} (1 - \zeta^{-1})^s \tag{B.20}$$

where the coefficients

$$\sigma_j^{(M)} = T_{M-1-j}^{(M)}, \qquad 0 \le j \le M-1 \tag{B.21}$$

are tabulated in Table II. A residue of this form is calculated for each pole $\zeta = \zeta_k$, and the result is the expression (3.16) for the probability Q_n^+.

REFERENCES

1. W. Feller, "An Introduction to Probability Theory and Its Applications," vol. 1, p. 478, Wiley, New York, 1966.
2. M. Teich, Applied Optics 20 (1981), 2457.
3. S. O. Rice, SIAM J. Sci. Stat. Comput. 1 (1980), 438.
4. C. W. Helstrom, SIAM J. Sci. Stat. Comput. 4 (1983) (in press).
5. H. E. Daniels, Ann. Math. Statist. 25 (1954), 631.
6. D. Blackwell, J. L. Hodges, Jr., Ann. Math. Statist. 30 (1959), 1113.
7. R. R. Bahadur, R. Ranga Rao, Ann. Math. Statist. 31 (1960), 1015.
8. V. V. Petrov, Th. Prob. and its Appl. 10 (1965), 287.
9. O. Barndorff-Nielsen, D. R. Cox, J. Roy. Stat. Soc. B, 41 (1979), 279.
10. H. T. Van Trees, "Detection, Estimation, and Modulation Theory," vol. 3, p. 39, Wiley, New York, 1971.
11. C. W. Helstrom, Trans. IEEE AES-14 (1978), 630.
12. S. O. Rice, Bell System Tech. J. 47 (1968), 1971.
13. F. A. Haight, "Handbook of the Poisson Distribution," p. 45, Wiley, New York, 1967.
14. J. Riordan, "An Introduction to Combinatorial Analysis," pp. 19-49, Wiley, New York, 1958.
15. M. Abramowitz, I. Stegun, "Handbook of Mathematical Functions," p. 257, Appl. Math. Series 55, U.S. Government Printing Office, Washington, D.C., 1964.
16. C. W. Helstrom, Proc. Phys. Soc. (London) 83 (1964), 777.
17. A. J. F. Siegert, Trans. IRE, IT-3 (1957), 38.
18. G. Bédard, Phys. Rev. 151 (1966), 1038.
19. G. Bédard, J. C. Chang, L. Mandel, Phys. Rev. 160 (1967), 1496.
20. J. Neyman, Ann. Math. Statist. 10 (1939), 35.

21. C. W. Helstrom, Trans. IEEE, AES-19 (1983) (in press).

22. G. F. Carrier, M. Krook, C. E. Pearson, "Functions of a Complex Variable," p. 257, McGraw-Hill, New York, 1966.

23. R. Lugannani, S. O. Rice, J. Comp. Phys. 39 (1981), 473.

24. S. O. Rice, Bell System Tech. J. 52 (1973), 707.

25. R. Lugannani, S. Rice, Adv. Appl. Prob. 12 (1980), 475.

26. K. Knopp, "Theorie und Anwendung der unendlichen Reihen," 2nd ed., p. 315, Springer, Berlin, 1924.

Table I

Performance of Residue Series for Q_n^+ (40 terms)

Lorentz spectral density, m = 4.4365821

	$N_p = 5$, $G = 20$				$N_p = 20$, $G = 5$		
n	Residue series	Exact	Last increment	n	Residue series	Exact	Last increment
20	0.940032	0.939034	2.20(-3)	20	0.991725	0.991717	6.38(-6)
40	0.842027	0.842012	2.40(-5)	40	0.928487	0.928483	3.60(-10)
60	0.710186	0.710182	3.45(-7)	60	0.785282	0.785280	2.03(-14)
80	0.567215	0.567213	6.71(-9)	80	0.602037	0.602037	1.14(-18)
100	0.433256	0.433255	1.25(-10)	100	0.428268	0.428268	6.43(-23)

Table II

Coefficients $\sigma_j^{(M)}$ in (3.16)

M	0	1	2	3	4	5	6	7	8	9	10	11
1	1											
2	1	1										
3	1	$\frac{3}{2}$	1									
4	1	$\frac{11}{16}$	2	1								
5	1	$\frac{25}{12}$	$\frac{35}{12}$	$\frac{5}{2}$	1							
6	1	$\frac{137}{60}$	$\frac{15}{4}$	$\frac{17}{4}$	3	1						
7	1	$\frac{49}{20}$	$\frac{203}{45}$	$\frac{49}{8}$	$\frac{35}{16}$	$\frac{7}{2}$	1					
8	1	$\frac{363}{140}$	$\frac{469}{90}$	$\frac{967}{120}$	$\frac{28}{3}$	$\frac{23}{3}$	4	1				
9	1	$\frac{761}{28}$	$\frac{29531}{5040}$	$\frac{801}{80}$	$\frac{1069}{80}$	$\frac{27}{2}$	$\frac{39}{4}$	$\frac{9}{2}$	1			
10	1	$\frac{7129}{252}$	$\frac{6515}{1008}$	$\frac{4523}{378}$	$\frac{285}{16}$	$\frac{3013}{144}$	$\frac{75}{4}$	$\frac{145}{12}$	5	1		
11	1	$\frac{7381}{2520}$	$\frac{177133}{25200}$	$\frac{84095}{6048}$	$\frac{341693}{1512}$	$\frac{8591}{288}$	$\frac{7513}{240}$	$\frac{605}{24}$	$\frac{44}{3}$	$\frac{11}{2}$	1	
12	1	$\frac{83711}{27720}$	$\frac{190553}{25200}$	$\frac{103344293}{6531840}$	$\frac{1254429}{45360}$	$\frac{242537}{6048}$	$\frac{1901}{40}$	$\frac{10831}{240}$	33	$\frac{35}{2}$	6	1

Table III

Performance of Residue Series (3.16) for Q_n^+

Negative-Binomial Primary Distribution (M = 5)

n	Single term	Residue series	Num	Exact
	$N_p = 5, \quad G = 20$			
20	0.932417	0.955457	4	0.955457
40	0.833080	0.873738	3	0.873737
60	0.705184	0.749536	2	0.749535
80	0.568492	0.601921	2	0.601920
100	0.439202	0.439582	2	0.439582
150	0.198436	0.198413	2	0.198413
200	0.0763843	0.0763844	2	0.0763845
	$N_p = 20, \quad G = 5$			
20	0.983799	0.983798	1	0.983799
40	0.911155	0.911153	1	0.911155
60	0.775914	0.775912	1	0.775914
80	0.608256	0.608256	1	0.608258
100	0.443583	0.443581	1	0.443583
150	0.157956	0.157956	1	0.157956
200	0.0440489	0.0440489	1	0.0440489

Table IV

Q_n^-: Neyman Type-A Distribution

Numerical Contour Integration

n	Number of steps	y_0	Result of integration	Exact
		$N_p = 5, \quad G = 20$		
25	37	1.687	3.5527190(-2)	
	74	1.687	3.5523618(-2)	
	148	1.687	3.5523618(-2)	3.5523618(-2)
100	36	0.6551	0.52720529	
	71	0.6460	0.52698250	
	141	0.6415	0.52698245	0.52698245
175	36	0.5099	1-6.3492573(-2)	
	71	0.5029	1-6.3492302(-2)	
	141	0.4993	1-6.3492302(-2)	1-6.3492302(-2)
		$N_p = 20, \; G = 5$		
25	41	2.856	9.3933963(-5)	
	82	2.856	9.3933799(-5)	
	164	2.856	9.3933799(-5)	9.3933799(-5)
100	30	0.9178	0.51061370	
	60	0.9178	0.51045010	
	120	0.9178	0.51045007	0.51045007
175	25	0.7618	1-2.9833051(-3)	
	50	0.7618	1-2.9833045(-3)	
	99	0.7542	1-2.9833045(-3)	1-2.9833046(-3)

Table V

Q_n^+: Distribution Generated by Negative-Binomial, M = 5

Numerical Contour Integration

n	Number of steps	y_0	Result of integration	Exact
		Np = 5, G = 20		
25	30	1.3191	1-9.7678911(-2)	
	60	1.3191	1-9.7652467(-2)	
	119	1.3081	1-9.7652467(-2)	1-9.7652465(-2)
100	71	0.5602	0.43963053	
	143	0.5563	0.43958206	
	285	0.5543	0.43958206	0.43958206
175	57	0.4193	0.12519049	
	115	0.4157	0.12518192	
	229	0.4157	0.12518192	0.12518192
		N_p = 20, G = 5		
25	22	1.3094	1-2.7957485(-2)	
	43	1.2796	1-2.7954584(-2)	
	84	1.2647	1-2.7954585(-2)	1-2.7954583(-2)
100	55	0.5571	0.44363275	
	112	0.5571	0.44358254	
	223	0.5571	0.44358254	0.44358255
175	47	0.4211	8.5479092(-2)	
	94	0.4211	8.5472726(-2)	
	187	0.4188	8.5472726(-2)	8.5472739(-2)

Table VI

Saddlepoint Approximations

Q_n^-: Neyman Type-A

$N_p = 5, \quad G = 20$

n	UAE	Off-axis contribution	Total	Exact	Crude S-P
25	3.14560(-2)	4.09137(-3)	3.55474(-2)	3.55236(-2)	3.289(-2)
50	0.130576	9.51063(-6)	0.130585	0.130600	0.1324
100	0.527499	-5.51718(-4)	0.526947	0.526982	0.5103
150	0.857731	3.01480(-5)	0.857762	0.857777	0.8626
200	1-2.50472(-2)	9.23185(-7)	1-2.50463(-2)	1-2.50431(-2)	1-2.478(-2)

$N_p = 18, \quad G = 72$

250	1.98051(-5)	-1.71780(-6)	1.80873(-5)	1.80638(-5)	2.022(-5)
500	1.81082(-3)	1.81503(-5)	1.82897(-3)	1.82849(-3)	1.826(-3)
750	2.98581(-2)	5.45979(-5)	2.99127(-2)	2.99100(-2)	2.986(-2)
1000	0.168343	-2.72697(-4)	0.168070	0.168064	0.1657
1500	0.752654	-8.41239(-5)	0.752570	0.752567	0.7648
2000	1-1.58622(-2)	-2.85533(-7)	1-1.58625(-2)	1-1.58627(-2)	1-1.571(-2)

Table VII

Saddlepoint approximations

Q_n^-: Distribution Arising from Negative-Binomial, M = 5

$N_p = 5, \quad G = 20$

n	UAE	Off-axis contribution	Total	Exact	Crude S-P
25	8.87698(-1)	8.93627(-3)	9.77061(-2)	9.75652(-2)	9.260(-2)
50	0.228548	1.32791(-3)	0.229876	0.229878	0.2324
100	0.560734	-3.80191(-4)	0.560354	0.560418	0.6189
150	0.801492	2.28596(-5)	0.801515	0.801587	0.8156
200	1-7.64312(-2)	-1.88311(-7)	1-7.64314(-2)	1-7.63845(-2)	1-7.375(-2)

$N_p = 18, \quad G = 72$

250	1.50326(-2)	1.09488(-5)	1.50435(-2)	1.50203(-2)	1.539(-2)
500	8.17995(-2)	-4.29986(-4)	8.13695(-2)	8.13251(-2)	8.292(-2)
750	0.208630	4.65397(-4)	0.209096	0.209060	0.2101
1000	0.369655	-2.76864(-4)	0.369378	0.369373	0.3692
1500	0.672094	-3.98353(-5)	0.672054	0.672103	0.7066
2000	0.860206	-2.67366(-6)	0.860204	0.860256	0.8678

FIGURE CAPTIONS

Fig. 1. Probability distributions $\{p_n\}$ of secondary electrons when the primary electrons have negative-binomial distributions (solid lines) or arise from incident light with a Lorentz spectral density (dashed lines); $N_p = 2$, $G = 6$. The curves are indexed by the number M of degrees of freedom. The curve marked '∞' represents the Neyman Type-A distribution.

Fig. 2. Probability distributions $\{p_n\}$ of secondary electrons when the primary electrons have negative-binomial distributions (solid lines) or arise from incident light with a Lorentz spectral density (dashed lines); $N_p = 6$, $G = 2$. The curves are indexed by the number M of degrees of freedom. The curve marked '∞' represents the Neyman Type-A distribution.

Fig. 3. Paths of steepest descent of the integrands in (1.7) and (1.8) when the cumulative Neyman Type-A distribution is being calculated for $N_p = G = 10$. The left-hand curve is for $n = 75$, the right-hand for $n = 150$. The small circles indicate the saddlepoints of the integrand.

Fig. 4. Cumulative distributions of the number of secondary electrons when the primary electrons have a negative-binomial distribution; $N_p = 5$, $G = 20$. The curves are indexed by the number M of degrees of freedom, the curve marked '∞' representing the Neyman Type-A distribution. The small circles denote values of the cumulative distribution when the incident light has a Lorentz spectral density with the same number of degrees of freedom.

Fig. 5. Cumulative distributions of the number of secondary electrons when the primary electrons have a negative-binomial distribution; $N_p = 20$, $G = 5$. The curves are indexed by the number M of degrees of freedom, the curve marked '∞' representing the Neyman Type-A distribution. The small circles denote values

of the cumulative distribution when the incident light has a Lorentz spectral density with the same number of degrees of freedom.

Fig. 6. Cumulative distributions of the number of secondary electrons when the primary electrons have a negative-binomial distribution; $N_p = 18$, $G = 72$. The curves are indexed by the number M of degrees of freedom, the curve marked '∞' representing the Neyman Type-A distribution. The small circles denote values of the cumulative distribution when the incident light has a Lorentz spectral density with the same number of degrees of freedom.

Fig. 7. Cumulative distributions of the number of secondary electrons when the primary electrons have a negative-binomial distribution; $N_p = 72$, $G = 18$. The curves are indexed by the number M of degrees of freedom, the curve marked '∞' representing the Neyman Type-A distribution. The small circles denote values of the cumulative distribution when the incident light has a Lorentz spectral density with the same number of degrees of freedom.

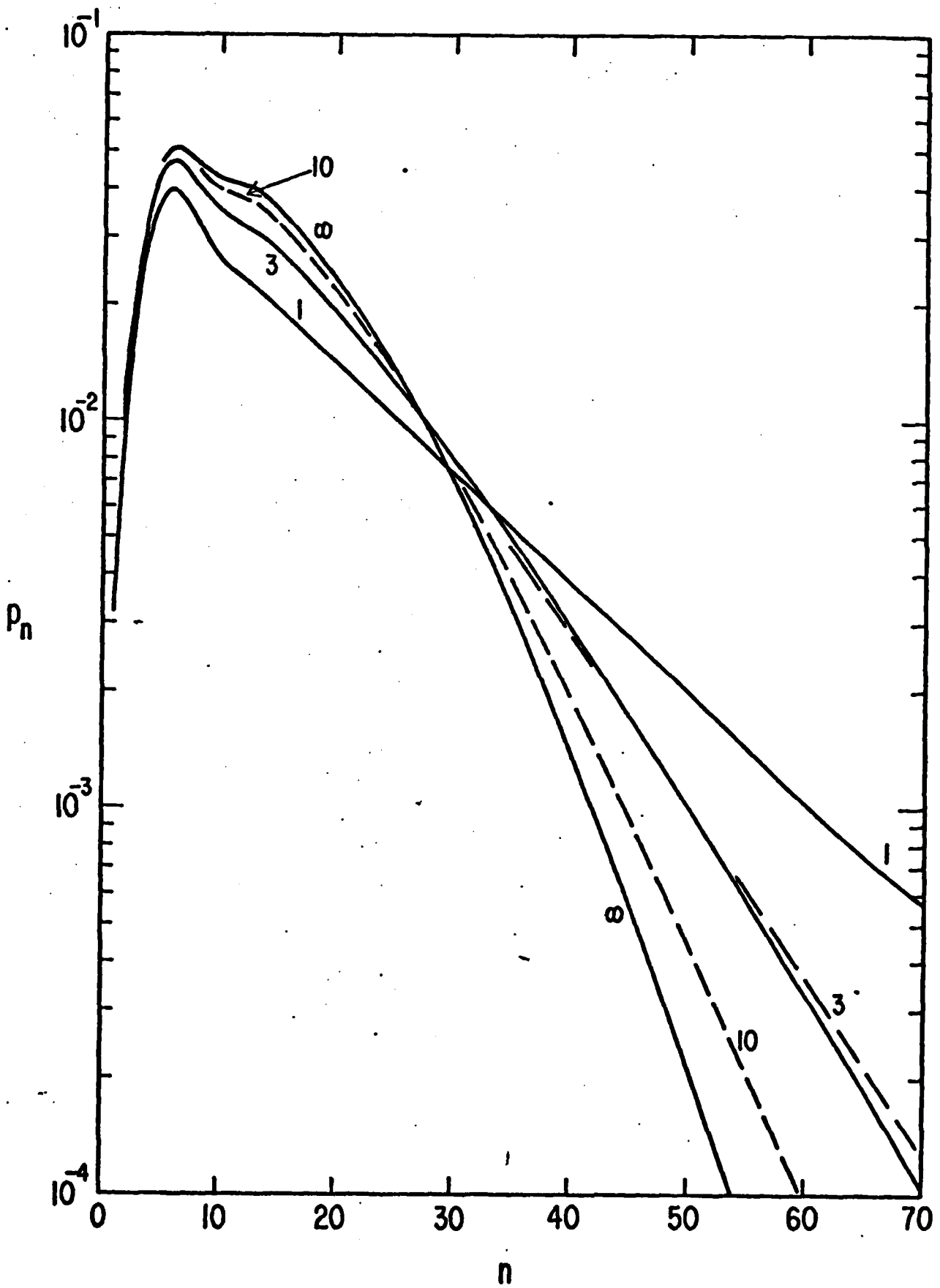

Fig. 1

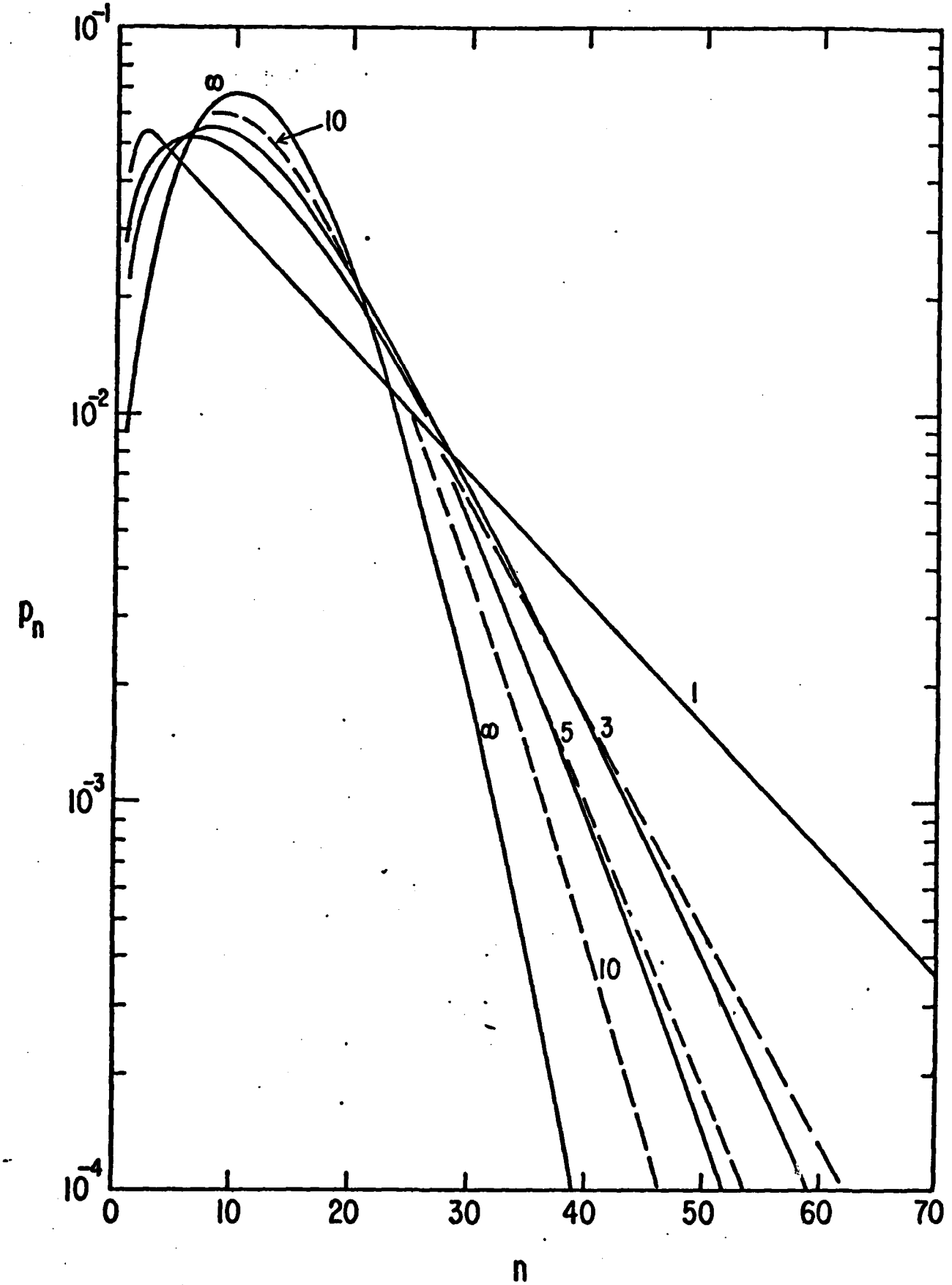

Fig. 2

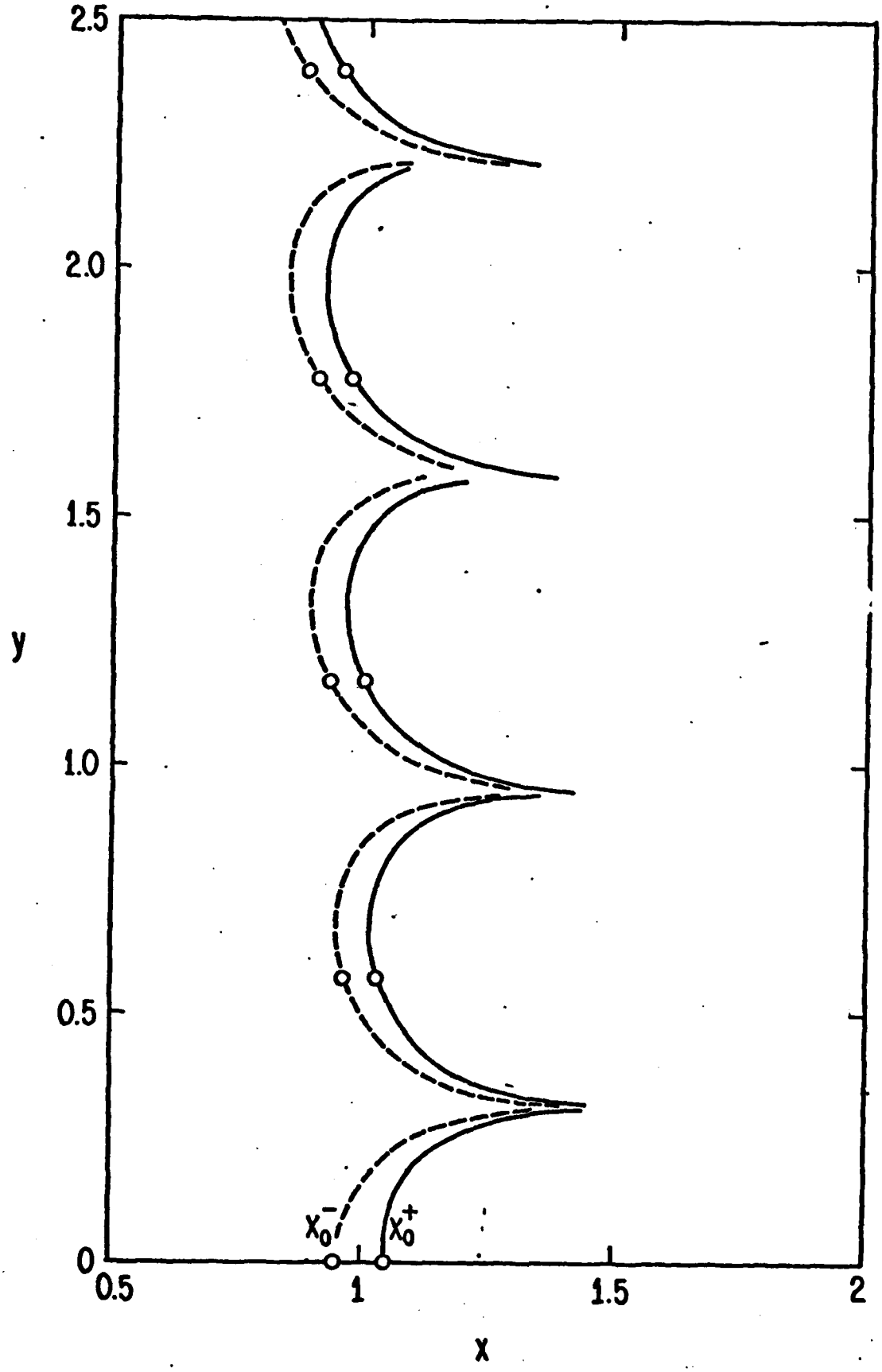

Fig. 3

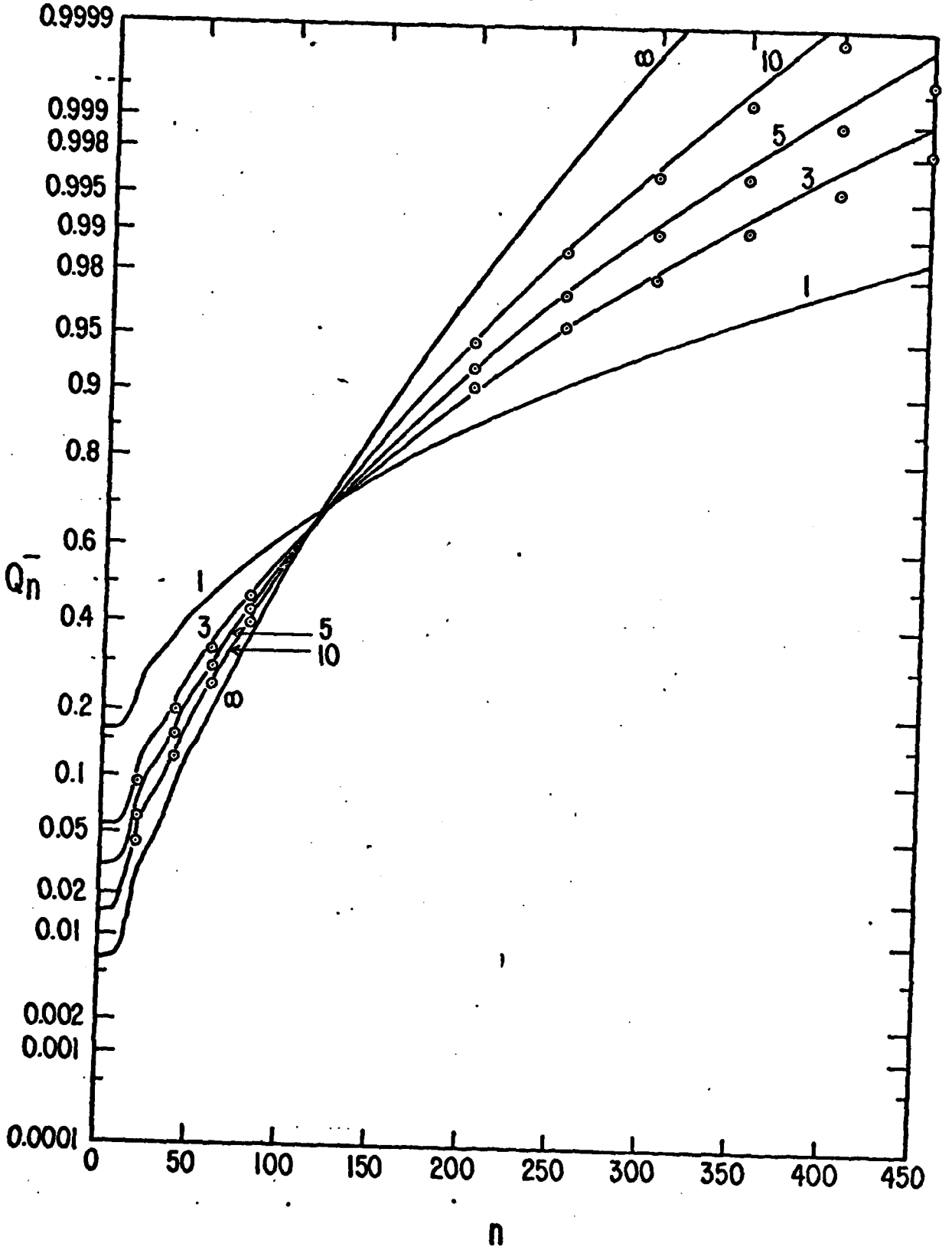
0.9999
0.999
0.998
0.995
0.99
0.98
0.95
0.9
0.8
0.6
0.4
0.2
0.1
0.05
0.02
0.01
0.002
0.001
0.0001
Q_n^-
0
50
100
150
200
250
300
350
400
450
n
∞
10
5
3
1
1
3
5
10
∞

Fig. 4

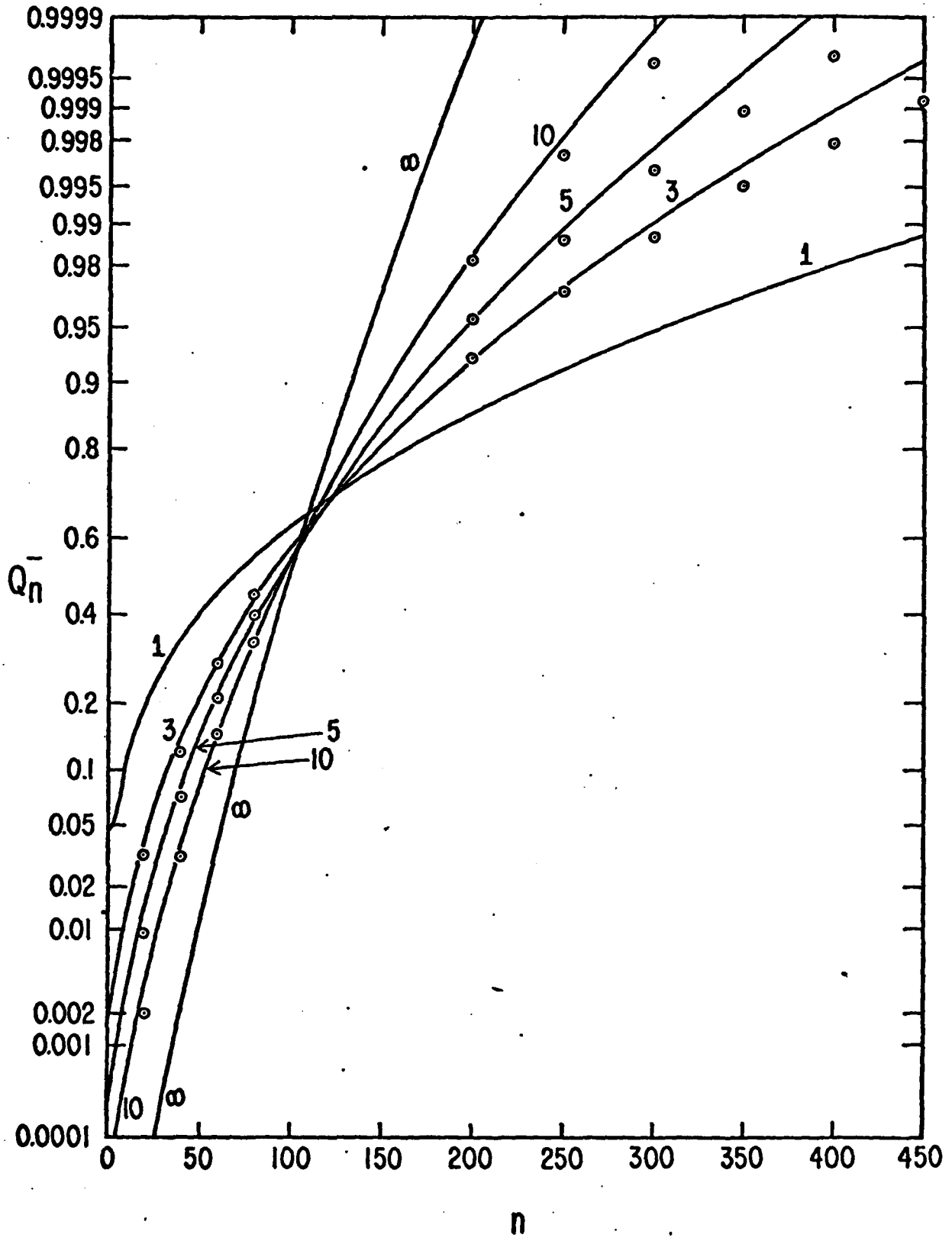
0.9999
0.9995
0.999
0.998
0.995
0.99
0.98
0.95
0.9
0.8
0.6
0.4
0.2
0.1
0.05
0.02
0.01
0.002
0.001
0.0001
Q_n^-
0
50
100
150
200
250
300
350
400
450
n
∞
10
5
3
1
1
3
5
10
∞
10
∞

Fig. 5

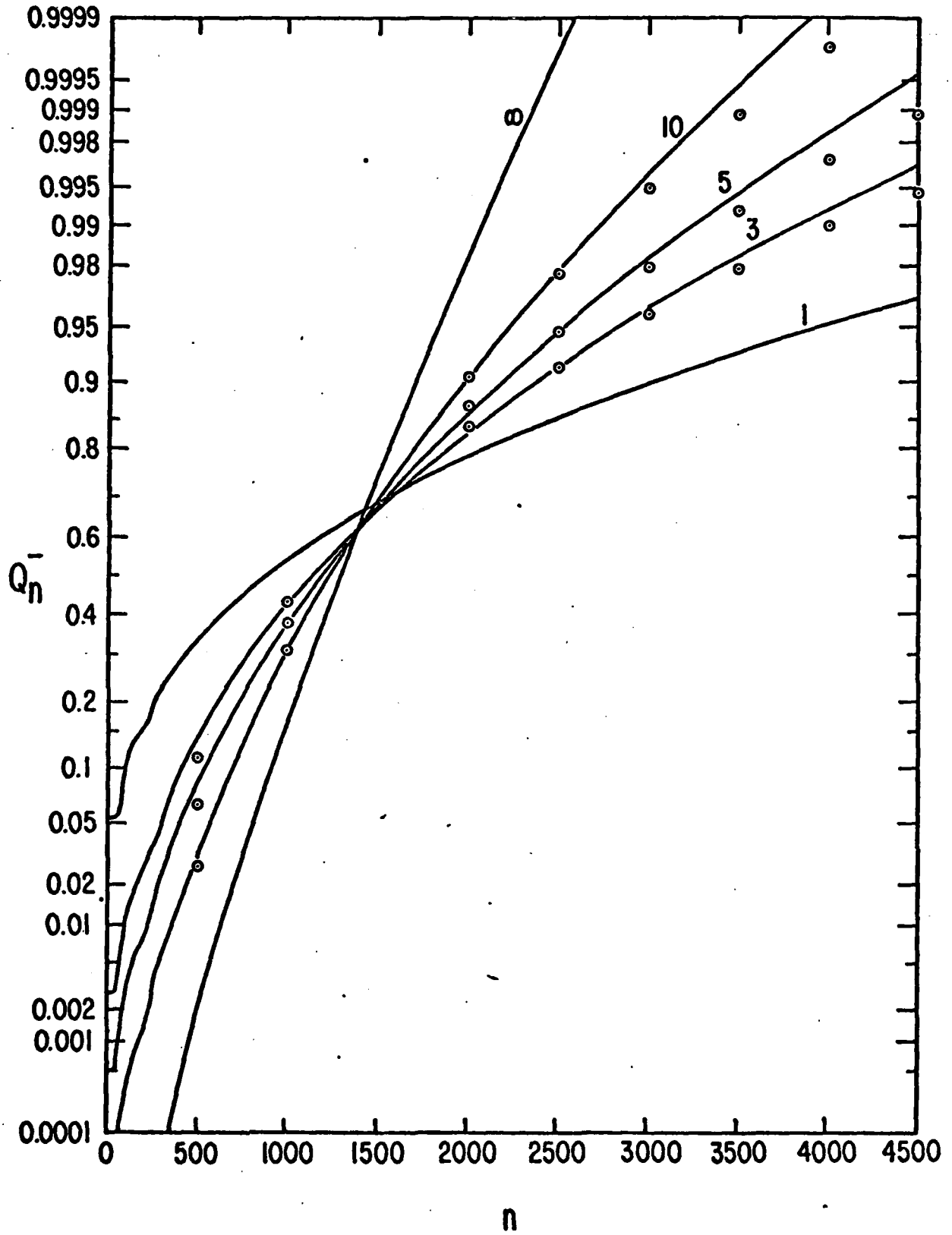
0.9999
0.9995
0.999
0.998
0.995
0.99
0.98
0.95
0.9
0.8
0.6
0.4
0.2
0.1
0.05
0.02
0.01
0.002
0.001
0.0001
Q_n^-
0
500
1000
1500
2000
2500
3000
3500
4000
4500
n
∞
10
5
3
1

Fig. 6

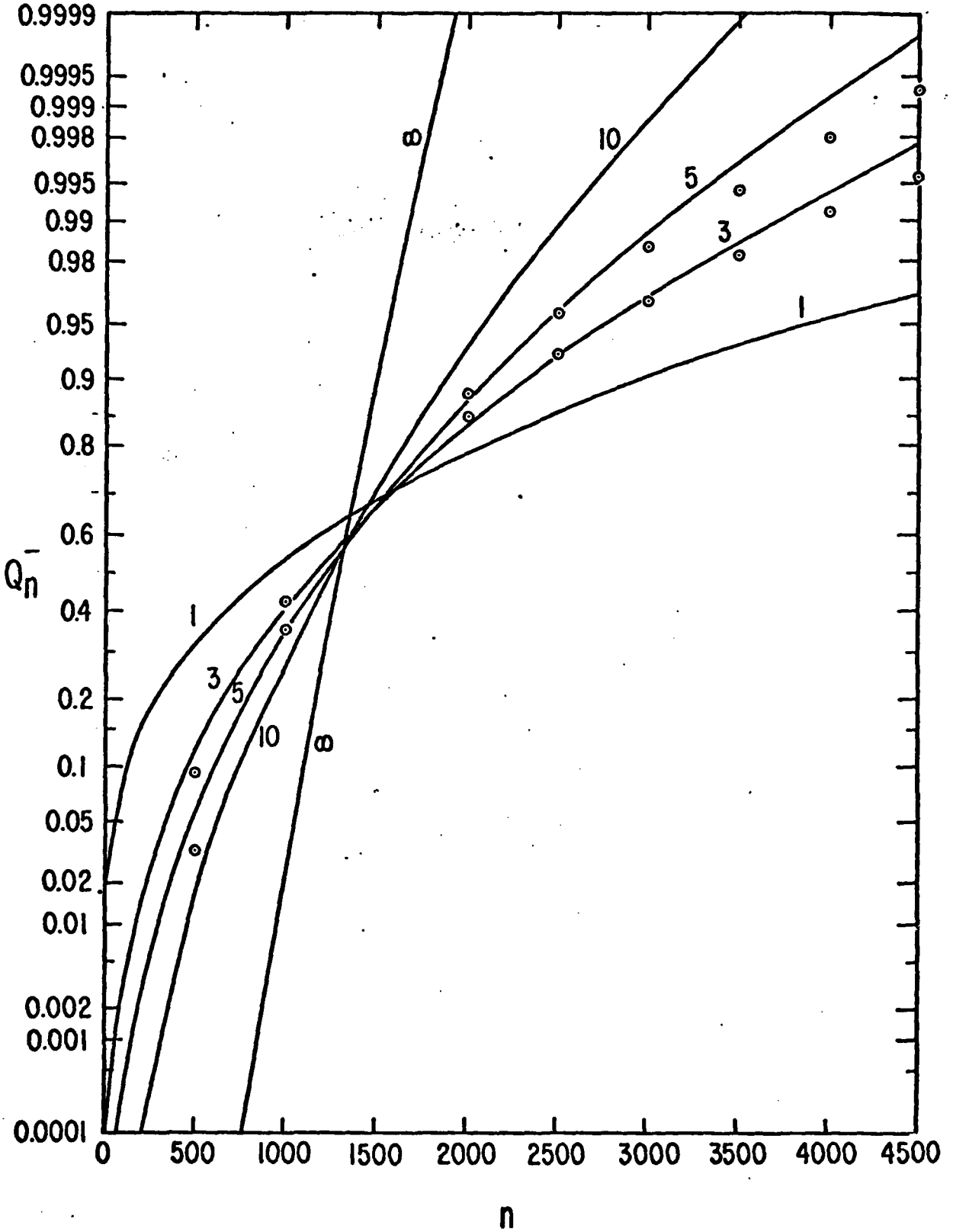
0.9999
0.9995
0.999
0.998
0.995
0.99
0.98
0.95
0.9
0.8
0.6
0.4
0.2
0.1
0.05
0.02
0.01
0.002
0.001
0.0001
Q_n^-
0
500
1000
1500
2000
2500
3000
3500
4000
4500
n
∞
10
5
3
1
1
3
5
10
∞

Fig. 7

END

FILMED

9-83

DTIC